Expression and Characterization of a Bright Far-red Fluorescent Protein from the Pink Pigmented Tissues of *Porites lobata*

Mary C. Bridges[1,2,3], Cheryl M. Woodley[2*], Esther C. Peters[4], Lisa A. May[5], Sylvia B. Galloway[2]

[1] Formerly of the Graduate Program in Marine Biology, College of Charleston, Charleston, South Carolina, USA
[2] National Centers for Coastal Ocean Science Charleston Laboratory, NOS, NOAA, Charleston, South Carolina, USA
[3]Currently in the Department of Regenerative Medicine and Cell Biology, Medical University of South Carolina, Charleston, South Carolina, USA
[4] Department of Environmental Science & Policy, George Mason University, Fairfax, Virginia, USA
[5] Consolidated Safety Services, Inc. contractor at Center for Coastal Environmental Health and Biomolecular Research, NCCOS, NOS, NOAA, Charleston, South Carolina, USA

***** Corresponding author
E-mail: cheryl.woodley@noaa.gov
Phone: 843-460-9805

Funding Information: NOAA's Coral Reef Conservation Program Project # 1133.

ORCIDs:
M.C. Bridges: 0000-0003-1101-0848
C.M. Woodley: 0000-0001-7532-2934
E.C. Peters: 0000-0001-5404-5309
L.A. May: 0000-0002-5050-1474

Abstract

Members of the anthozoan green fluorescent protein (GFP) family display a diversity of photo-physical properties that can be associated with normal and damaged coral tissues. Poritid coral species often exhibit localized pink pigmentation in diseased or damaged tissues. Our spectral and histological analyses of pink pigmented *Porites lobata* lesions shows co-localization of bright red fluorescence with putative amoebocytes concentrating in the epidermis, suggesting an activated innate immune response. Here we report the cloning, expression, and characterization of a novel red fluorescent protein (plobRFP) from the pink-pigmented tissues associated with lesions on *Porites lobata*. *In vitro*, the recombinant plobRFP exhibits a distinct red emission signal of 614 nm (Ex. max: 578 nm), making plobRFP the furthest red-shifted natural fluorescent protein isolated from a scleractinian coral. The recombinant protein has a high molar extinction coefficient (84,000 $M^{-1}cm^{-1}$) and quantum yield (0.74), conferring a notable brightness to plobRFP. Sequence analysis suggests the distinct brightness and marked red shift may be inherent features of plobRFP's chromophore conformation. While plobRFP displays a tendency to aggregate, its high pH stability, photostability, and spectral properties make it a candidate for cell imaging applications and a potential template for engineering optimized RFPs. The association of plobRFP with a possible immune response furthers its potential use as a visual diagnostic and molecular biomarker for monitoring coral health.

Keywords (4-6): red fluorescent protein (RFP); coral innate immune response; *Porites lobata*; tissue pigmentation response (TPR)

Introduction

Members of the green fluorescent protein (GFP) superfamily possess chromophoric structures synthesized directly from their polypeptide chains and are capable of producing fluorescent emission signals auto-catalytically (Heim et al. 1994). This autocatalysis has facilitated their use as genetically encoded fluorescent probes in a wide variety of *in vivo* as well as *in situ* imaging applications (Chudakov et al. 2010; Stepanenko et al. 2011). Currently, anthozoan species represent the largest known natural repository for members of this fluorescent protein superfamily (Ong et al. 2011) with GFP-like proteins emitting along the entire visible spectrum, have been cloned and characterized from corals (Matz et al. 1999; Labas et al. 2002; Alieva et al. 2008).

Fluorescent protein (FP) emission wavelength and brightness are influenced directly by the tripeptide combination that forms the fluorescent protein's chromophoric structure, as well as its interactions with surrounding amino acid residues (Nienhaus and Wiedenmann 2009). Chromophore formation involves the cyclization of the polypeptide backbone to form an imidazolinone ring, followed by spontaneous oxidation and dehydration steps that extend the π-conjugation system of the chromophore (Heim et al. 1994; Tsien 1998). In most red and orange emitting FPs, the conjugated π-electron system is further extended by an additional oxidation step (Wall et al. 2000; Gross et al. 2000; Yarbrough et al. 2001), facilitating a red-shift in emission. All members of the GFP-like superfamily form into a rigid β-barrel shape (composed of 11 β-strands) surrounding the chromophore moiety (Yang et al. 1996; Ormo et al. 1996). Variation in amino acids at key positions along the polypeptide chain influences the environment within the β-barrel and tune FP emission signals.

As mutations in the FP gene directly translate into changes in the polypeptide sequence and consequently spectral properties, the molecular evolution of FP color variety in coral species has been explored by phylogenetic studies, revealing that scleractinian coral color diversity most likely arose from a common green ancestral fluorescent protein (Alieva et al. 2008; Ugalde et al. 2004). It is generally thought that the more molecularly complex red and cyan-emitting fluorescent proteins are the result of multiple convergent evolutionary events (Alieva et al. 2008; Shagin et al. 2004), and their non-green emission signals were likely shaped and preserved by positive natural selection (Field et al. 2006). This evokes unanswered questions regarding the biological role of fluorescent proteins in anthozoan species. Most well-known hypotheses about the functional role of coral FPs focus on the symbiotic relationship that exists between the coral host and zooxanthellae, suggesting that FPs may play a light enhancing or photoprotective role (Kawaguti 1969; Dove et al. 2001; Salih et al. 2000). These hypotheses, however, do not explain the diversity of colors represented, the discovery of FPs in azooxanthellate species (Wiedenmann et al. 2004; Vogt et al. 2008), nor the emission/absorption profiles of many FPs (particularly RFPs) that would contribute minimally to efficient symbiont photosynthesis or photoprotection (D'Angelo et al. 2008; Levy et al. 2003). Therefore, it is likely that individual FPs or different groups of FPs play distinct functional roles in coral species.

An induced pigmentation response in the scleractinian coral species*, Porites* (pink pigmentation) and *Acropora* (purple-blue pigmentation), has been described by a number of investigators (Ravindran and Raghukumar 2006; Aeby 2003; Benzoni et al. 2010; Bongiorni and Rinkevich 2005; Palmer et al. 2008). This response, induced by physical damage or pathogen

infection, disrupting coral tissue integrity, has been characterized as an innate immune response due to histological observations of putative amoebocytes and evidence of phenoloxidase (PO)-activating melanin synthesis in the pigmented tissues of these species (Palmer et al. 2008; D'Angelo et al. 2012). This reaction is thought to be similar to an invertebrate inflammation response involving the phagocytosis of cellular debris and pathogens with a melanin barrier formation. Palmer et al. (2009a,b) proposed that GFP-like proteins in the pigmented tissues of *Acropora* and *Porites* species may also function as antioxidants, since reactive oxygen species (ROS) are a byproduct of the PO-activating melanin synthesis pathway and FPs are capable of scavenging ROS (Bou-Abdallah et al. 2006; Shikina et al. 2016). Increased proliferation in these pigmented tissues has also been observed, suggesting an association of this pigmentation response with the regeneration/wound healing phase of the coral innate immune response (D'Angelo et al. 2012). The induction of a localized red fluorescent signal in the pink-pigmented tissues of *Porites* spp. is unique. In other coral species, red fluorescence is most often observed uniformly throughout healthy coral tissues or localized to anatomical regions, such as the tentacle tips and oral pores of anemones (Gruber et al. 2008; Ikmi and Gibson 2010; Oswald et al. 2007). The distinct presence of red fluorescence in compromised tissues, typically exhibiting a uniform green fluorescent signal, distinguishes *Porites* RFPs and offers support for a specialized functional role.

A red fluorescent protein (pporRFP) with an emission maximum of 596 nm has been cloned and characterized from *Porites porites* (Alieva et al. 2008). Palmer et al. (2009b) reported a similar emission profile from the pink-pigmented tissues of *Porites compressa* and suggested that pporRFP was characteristic of *Porites* spp. However, it is significant to note that the emission signal recorded from the pink-pigmented tissues of *Porites lobata* reported here, is distinct and shifted much further into the red (Em. max: 614) than the RFPs previously described from other *Porites* spp.

In this study, we clone, express, and characterize the RFP (plobRFP) associated with the pink tissue pigmentation response of *Porites lobata*. The cloning of plobRFP provides the opportunity to examine sequence divergence between two closely related, but spectrally unique RFPs (pporRFP and plobRFP) and adds another member to a subset of FPs with a potentially distinct biological role in a coral immune response. Furthermore, plobRFP represents the furthest red-shifted natural fluorescent protein isolated from a scleractinian coral and its distinct brightness sets plobRFP apart from other naturally occurring far-red emitting FPs, which suffer from diminished brightness.

Materials and Methods

Porites lobata sample collection

Approximately 1 g of tissue with minimal skeletal contamination was collected from the pink-pigmented region bordering a circular lesion of a *Porites lobata* specimen held in aquaculture (in artificial seawater, 34 ppt; 8 h light-16 h dark light cycle, at 26 °C) at the NOS NCCOS Charleston Laboratory, Coral Culture Facility (Charleston, SC). The tissue sample was immediately frozen in liquid nitrogen and used for the construction of a cDNA expression library.

Histology

A second tissue sample from a *Porites lobata* specimen displaying the pink tissue pigmentation response was collected for histology and fixed in a solution of 1 part Z-Fix concentrate (Anatech) diluted with 1 part 70 ppt artificial seawater (Sigma), and 3 parts 35 ppt artificial seawater to make 2X Z-Fix; sea salts were dissolved in Type I water. The sample was decalcified in 10% disodium ethylenediaminetetraacetic acid (Na_2EDTA), pH 7.4, and stored in 70% ethanol. Following decalcification, the tissue sample was trimmed (~2 cm x 0.7 cm) and paraffin embedded for cross-sectional and sagittal views of the polyps. Tissues were sectioned for light (5 µm thick) and confocal (10 µm thick) microscopy. Sections were stained with either Harris' hematoxylin and eosin (HH&E) (nuclei and cytoplasm), Mallory's trichrome (collagen), Gomori's methenamine-silver (GMS) (fungi), Fontana-Masson (melanin-like pigments), or periodic acid-Schiff reagent procedures (PAS) (polysaccharides, mucins, glycoproteins).

cDNA library construction and screening

The cDNA expression library was prepared commercially (Express Genomics, Frederick, MD) following a proprietary protocol. Briefly, total RNA was isolated from the homogenized coral tissue sample using TRIzol® Reagent and poly(A)+RNA transcripts were separated from total RNA by two rounds of selection with oligo(dT)-coated magnetic particles. The cDNA library was constructed by using an oligo (dT) primer-adapter containing a *Not* I site and Moloney murine leukemia virus reverse transcriptase (M-MLV RT) to prime and synthesize the first strand cDNA. After the second strand was synthesized, the double stranded cDNA was size fractionated (>1.0 kb) and cloned directionally into the *Not* I and *Eco* RV sites of the proprietary pExpress1 eukaryotic expression vector; primary clones from one ligation reaction were electroporated into T1 phage resistant *E. coli*. The primary library was expanded by gentle culture in a semi-solid agarose matrix.

The plasmid DNA from the cDNA library was screened by PCR for GFP-like coding sequences. Degenerate primers were designed to homologous, conserved regions of sequence identified from a multiple alignment, constructed with the coding sequences of DsRed type fluorescent proteins and chromoproteins comprising Clade B of the coral FP molecular phylogeny constructed by Alieva et al. (2008). Several degenerate primer combinations (Online Resource 1, Table S.1) were used (in combination with each other or the vector-anchored primer M13F: 5'-CCC AGT CAC GAC GTT GTA AAC G-3') to amplify, sub-clone, and sequence segments of the RFP-like protein coding sequence.

The largest resulting segment of the FP coding sequence was used to design 'capture and blocking' oligonucleotides for the magnetic bead capture technique previously described by Shepard and Rae (1997). In summary, a shorter 5' biotinylated probe, 5'-TAC AGT CAC TAA AGG TGC GCC T-3', was designed to bind to a portion of sequence near the 5' end of the known RFP coding sequence; two longer oligonucleotides, 5'-GAA GTG GAC AGC CTT ACG AGG GTG TGC AGA AAA TGA AGC T-3' and 5'-TTG CCA TTT TCT ATT GAC ATT TTG CTG CCT CAA GAA ATG-3', corresponding to the 5' and 3' (respectively) flanking regions of coding sequence adjacent to the biotinylated probe binding site were used as "blocking oligos." Approximately 5 µg (~9 x 10^{11} copies) of NaOH-denatured (0.1 N final concentration) plasmid DNA from the library was incubated with 80 ng of each oligonucleotide for 5 min at ~25 °C. The denaturation reaction was neutralized by the addition of Tris-hybridization buffer (6X Saline-Sodium Phosphate-EDTA **(**SSPE), 0.1% Tween 20, 50 mM Tris-HCl, pH7.4) and the mixture was incubated at 37 °C for 1 h.

At the end of the hybridization reaction, plasmids captured by the biotinylated oligonucleotide complexes were isolated with streptavidin-coated magnetic beads (30 min incubation, 25 °C, shaking); washed six times with wash buffer (6X SSPE, 0.1% Tween-20) and once with Type I water; re-suspended in 0.5X Tris-EDTA (TE) buffer; and eluted from the beads by heating at 80 °C for 3 min. Approximately 4 µl of captured plasmid DNA was used to transform One Shot® TOP10 Chemically Competent Cells (Life Technologies). Transformants were screened by colony PCR with primers flanking the multiple cloning site of the pExpress1 vector (M13F: 5'-CCC AGT CAC GAC GTT GTA AAC G-3' and M13R: 5'-AGC GGA TAA CAA TTT CAC ACA GG-3'). Clones containing inserts ≥ 750 bps in size were selected and then sequenced using the Sanger method (Sanger et al. 1977).

Expression and purification of *Porites lobata* RFP

Sequences of the selected clones were assembled using Sequencher 5.0 software (Gene Codes) and screened for complete open reading frames (ORFs). The gene identity of the ORFs was predicted by BLASTX (Altschul et al. 1990) searching the non-redundant protein database and resulted in the identification of a full length RFP-like coding sequence pulled directly from the cDNA expression library. For ease of manipulation, the FP coding insert was transferred into a vector to facilitate bacterial expression (the pGEM®-T Easy Vector, Promega). This required PCR amplifying the FP coding insert from the eukaryotic pExpress1 vector with primers that supplied features critical for recombinant protein expression and purification. The N-terminal primer included a 5' heel of 3 stop codons (translated in all 3 reading frames), a Shine-Dalgarno sequence (ribosome binding site to initiate bacterial translation of the FP coding sequence), a 6-base linker, and a portion of the coding sequence starting with the initiation codon (5'-TTG ATT GAT TGA AGG AGA AAT ATC ATG GCT CTT TCA AAG CAA ACT GGG-3'). The C-terminal (reverse) primer had a 5' heel with a 6-histidine tag (for protein purification) encoded in front of the stop codon, an alanine linker, and 25-bases corresponding to the antisense sequence of the FP-coding cDNA around the stop codon (5'-TTA TTA GTG ATG GTG ATG GTG ATG TGC TGC CTG ATT AAG GGA GTT GAG GCT AGA A-3'). The amplification products were purified using QIA Quick Gel Extraction Kit (QIAGEN), TA-cloned into the pGEM®-T Easy Vector, and transformed into One Shot® TOP10 Chemically Competent Cells according to the manufacturer's instructions.

Colonies exhibiting a faint pink color or dim red fluorescence, due to basal levels of expression, were inoculated into liquid cultures (LB broth supplemented with 100 µg/ml ampicillin, LB-Amp). Plasmids were purified from overnight cultures (grown at 37 °C) using a QIAprep Spin Miniprep Kit (QIAGEN) according to the manufacturer's protocol. These plasmids were subsequently transformed into XJb (DE3) Autolysis Z-Competent® Cells (Zymo Research), which are optimized for heterologous expression and in which recombinant protein production could be more tightly controlled.

These transformations were plated onto LB-Amp agar plates supplemented with 1 mM Isopropyl β-D-1-thiogalactopyranoside (IPTG) and grown overnight at 37 °C. Once colonies were visible, plates were held at 4 °C until pink color developed in the bacterial colonies (approximately 2-4 days). Visible pink colonies were first screened for red fluorescence with a fluorescent macroscope equipped with a long pass filter for 540 nm excitation (Olympus MVX-10), and then used to inoculate 10 mL starter cultures into LB-Amp broth. After growth overnight at 37 °C with shaking at 250 rpm, these starter cultures were transferred to larger

500 ml cultures of LB-Amp broth and grown to an optical density (O.D.) of ~0.6 measured at A=600 nm. While in exponential/log growth phase, expression was induced by the addition of IPTG to a final 1 mM concentration and cells were incubated at 20 °C overnight. Cells from these bacterial cultures were harvested by centrifugation (4,000 x *g,* 20 min, 4 °C), washed by re-suspension in phosphate buffered saline (PBS) (10 mM Na_2HPO_4, 2.7 mM KCl, 137 mM NaCl, 2 mM KH_2PO_4, pH 7.4), and pelleted by centrifugation (4,000 x *g,* 20 min, 4 °C). Cell pellets were stored at -80°C.

Thawed cell pellets were re-suspended in lysis buffer (50 mM NaH_2PO_4, 300 mM NaCl, 10 mM imidazole, 0.25% Tween-20, pH 8.0), sonicated on ice (six, 10 s bursts followed by a 10 s cooling period; amplitude: 20%), and centrifuged to remove cellular debris (10,000 x *g,* 30 min, 4 °C). The recombinant plobRFP product was purified from the cleared lysate using metal affinity chromatography on Ni-NTA agarose following the manufacturer's protocol (QIAexpress® System, QIAGEN). The recombinant RFP was eluted in 50 mM NaH_2PO_4, 300 mM NaCl, and 250 mM imidazole. The pure protein solution was concentrated to ~1.0 mg/ml and buffer exchanged into 50 mM NaH_2PO_4, 300 mM NaCl, 10 mM imidazole or PBS using a Centricon®-10 centrifugal filter device (EMD Millipore). Total protein concentration was estimated using a Micro BCA® Protein Assay Kit (Pierce Biotechnology).

Phylogenetic Analysis

The protein sequence of plobRFP was aligned with other anthozoan FPs using Clustal Omega (Sievers et al. 2011). The FPs chosen for analysis were selected from sequences previously used to construct a phylogenetic tree of anthozoan FPs created by Alieva et al. (2008) and a smaller phylogeny created by Ikmi and Gibson (2010). Three arthropod sequences served as an outgroup. The aligned FP sequences were subjected to phylogenetic analysis performed with MEGA6 (Tamura et al. 2013) (neighbor-joining method (Saitou and Nei 1987) with JTT matrix (Jones et al. 1992) and 1,000 bootstrap replications) or Geneious Prime 2019.2.3 (maximum likelihood using PhyML (Guindon and Gascuel 2003) with JTT matrix (Jones et al. 1992) and branch support calculated using an approximate likelihood ratio test (Chi2)).

Spectroscopic characterization

A BX-51 Olympus fluorescent microscope outfitted with a PARISS® hyperspectral spectrometer (Lightform) was used to record and compare fluorescent emission spectra collected from live coral specimens, bacterial cultures, and pure recombinant fluorescent protein solutions. The system was equipped with custom long-pass filter cubes with 430, 480, and 540 nm excitation filters as well as a narrower set with an excitation filter of 563-587 nm and an emission filter of 605-635 nm (Chroma Technology). Additional absorption, excitation, and emission spectra were recorded for the pure recombinant plobRFP solution. Absorption spectra were collected using a SPECTRAmax® PLUS^{384} microplate spectrophotometer; excitation and emission spectra were collected with a SPECTRAmax® GEMINI XS Dual Scanning microplate spectrofluorometer. Both instruments were equipped with SOFTmax PRO version 4.3 software (Molecular Devices).

The molar extinction coefficient (MEC) of the recombinant plobRFP at 578 nm (max excitation wavelength) was determined by the alkali-denaturation method (similar to that used by Alieva et al. (2008) and Shcherbo et al. (2007)). The absorption spectra of the native

chromophore (purified, recombinant plobRFP suspended in PBS) and the alkali-denatured chromophore (recombinant plobRFP solution diluted to an equal volume with 0.1N NaOH) were measured in quartz cuvettes with 1 cm pathlengths. It is known that at pH 13, the mature DsRed-like chromophore converts to a GFP-like chromophore that absorbs at 446 nm and has a MEC of 44,000 $M^{-1}cm^{-1}$ (Gross et al. 2000; Ward 2006). Using the absorption of the alkali-denatured plobRFP at 446 nm and the established MEC of alkali-denatured DsRed-like chromophores, the concentration of mature, functional chromophores present in the equally diluted native plobRFP recombinant protein solution was estimated. The estimated concentration of the functional plobRFP chromophore along with the absorbance value measured at 578 nm was used in the Beer-Lambert equation to calculate the MEC of the native plobRFP chromophore.

The fluorescence quantum yield (QY) of the plobRFP was determined at 25 °C relative to cresyl violet in methanol using the single-point method (Brouwer 2011; Lakowicz 2006). A range of dilutions (2 replicates for each dilution step) was prepared for the recombinant RFP (in PBS) and the QY reference standard, cresyl violet (in methanol) (Acros Organics). Absorption (350-650 nm) and emission (600-650 nm, excited at 546 nm) spectra were recorded for these dilutions in the same microtiter plate under identical conditions with 2 nm steps. Dilutions of plobRFP and cresyl violet with absorbances of 0.01, 0.02, 0.03, and 0.05 O.D. at the excitation wavelength of 546 nm were selected for QY calculations. Using the integrated fluorescence intensity from a plobRFP sample and reference sample at an identical concentration, a QY value for plobRFP was calculated relative to the known value of cresyl violet in methanol (QY: 0.54) (Magde et al. 1979; Isak and Eyring 1992). The calculated QY value was corrected for the refractive index difference between PBS (n: 1.337) and methanol (n: 1.3292). The final QY value for plobRFP reported here was established by taking the average of all the calculated single point QY values established for each of the three dilutions steps.

Oligomerization and aggregation

The oligomeric state of plobRFP was analyzed by standard discontinuous 12% (acrylamide: bis-acrylamide, 29:1) sodium dodecyl sulfate-polyacrylamide gel electrophoresis (SDS-PAGE) using SDS-Tris-glycine buffer (Laemmli 1970). Denatured protein samples (~1 µg of pure protein) were diluted in 5X SDS sample buffer (50% glycerol, 50 mM Tris, 10% SDS), heated at 95 °C for 4 min, and loaded directly onto the gel; pre-stained standard molecular weight markers (Blue Ranger® Marker Mix, Pierce) were used to estimate the sizes of the denatured proteins. To observe plobRFP in its pseudo-native state, protein samples (~1 µg of pure protein diluted in SDS sample buffer) were loaded directly (without heating) onto the gel. Migration of the un-heated sample was based on globular size while the heat-denatured sample was based on the linearized peptide. Unheated recombinant GFP (Vector Laboratories) and DsRed2 (Clontech) were used for globular size standards and served as monomeric and tetrameric size standards, respectively. Representative bands for pseudo-native protein samples were visualized immediately after electrophoresis, by their native fluorescence under UV illumination. Images were captured with a Gel Doc® XR+ imaging system (Bio-Rad) equipped with an ethidium bromide filter as well as a digital camera with no filter. The gel was then stained with Coomassie Brilliant Blue R (Sigma-Aldrich) and imaged with white light illumination using a G:Box Chemi HR16 imaging system (Syngene).

pH stability

To determine the chromophore sensitivity to pH, plobRFP samples were incubated and monitored for fluorescence in various pH buffers at 25 °C. The pH assay conducted was similar to those used by Hunt et al. (2010) and Masuda et al. (2006). Approximately 10 µg (10 µl) of the recombinant RFP (in 50 mM NaH_2PO_4, 300 mM NaCl, 10 mM imidazole) was added to 190 µl of buffer. Maximum fluorescent intensity (Ex: 578 nm; Em: 614 nm) and an absorbance spectrum were recorded immediately after the addition of the RFP sample and following a 20 min incubation at 25 °C using the microplate spectrophotometer/fluorometers described above. The pH buffers included: 0.1 M HCl (pH 1.26); 0.1 M glycine/HCl (pH 2.5 and 3.5); 0.1 M acetate buffer (pH 5); 0.1 M HEPES (pH 7); 0.1 M Tris/HCl (pH 8 and 9); 0.1 M carbonate (pH 11); 0.1 M NaOH (pH 13.5).

Photostability

The photostability of the recombinant plobRFP was determined as a measure of the time taken for the sample's emission maximum to drop to half the intensity of the initial fluorescence emission when exposed to intense illumination using an Olympus BX-51 fluorescent microscope equipped with a 540 nm long pass excitation filter. To maximize light intensity (light source: 200 W metal halide lamp), a 40X/0.9 W submersible objective was positioned above ~10 µl of a pure protein solution topped with mineral oil. The sample was exposed to continuous light while spectra were obtained once every millisecond and recorded using a screen image capture program (Camtasia, Tech Smith). Light intensity at the protein solution surface was measured using a submersible PAR Quantum Sensor (Skye Instruments) set up in similar fashion.

Results

Gross and histological observations of the pink tissue pigmentation response in *Porites lobata*

Porites lobata colonies in the laboratory developed focal or multifocal circular, subacute denuded skeletal lesions through slow mortality of polyps and coenenchyme on the surface or basally. An annular band of pink-pigmented tissue remained along the smooth to undulating lesion margin (Fig. 1a, e). Although appearing pink under white light, with blue/green light excitation it displayed brilliant red fluorescence in contrast to the green fluorescent pigments in "healthy" polyp and coenenchyme tissue (Fig. 1b, f). The purified pigment is shown in Fig. 1c and d with these same color characteristics. The denuded skeleton had fine filaments and sediment particles, but no other distinguishing features.

Histological observations of the pink-pigmented tissues of *P. lobata* showed a significant tissue response to a community of epi- or endolithic organisms in the denuded area and in the coenosteal skeleton between gastrovascular canals, including the concentration of granular melanin-containing cells within the epidermis and gastrodermis, specifically in regions flanking lysed tissue (Fig. 2a). In many areas, tissue beneath the surface body wall was fragmented and cells were necrotic or lysing with mucus filling the gastrovascular cavities and canals. Suspect filamentous bacteria and confirmed (by Grocott's methenamine silver and Periodic acid–Schiff staining) fungal hyphae infiltrated basal body wall epithelia; some cyanobacteria (based on morphology and Mallory's trichrome) and remnants of mesoglea, lysed coral cells, and organic

matrix were also seen in the denuded areas. The native fluorescence of the pink-pigmented tissue region was maintained throughout sample processing. In unstained sections of the pink pigmented tissues, the red fluorescence was localized to the epidermis (Fig. 2b); no red fluorescence was observed in the tissues distant from the lesion.

Cloning of a novel RFP

Using a homology-based PCR strategy followed by magnetic bead capture technique, the coding sequence of a novel red fluorescent protein, designated plobRFP (GenBank no. KM520152), was cloned from *Porites lobata* tissues exhibiting a distinct pink tissue pigmentation response. The full length plobRFP (GenBank no. AKM77632) is 233 amino acids with a calculated molecular weight of 26.5 kDa. The amino acid sequence displays 79% sequence identity with its closest homolog, pporRFP (GenBank no. ABB17953) (Alieva et al. 2008); ~65% identity with the *Acropora* chromoproteins, aacuCP, ahyaCP, and amilCP580 (GenBank no. AAU06856, AAU06855, AGH32877) (Alieva et al. 2008; Smith et al. 2013); and 61% identity with the red fluorescent/chromoprotein, eforCP/FP (GenBank no. ACD13196) (Alieva et al. 2008). The primary sequence of plobRFP shares less similarity to the representative coral DsRed-like fluorescent proteins DsRed (58%) (GenBank no. AAF03369) (Matz et al. 1999) and eqFP611 (50%) (GenBank no. AAN05449) (Wiedenmann et al. 2002) and to NvFP-7R (45%) (Ikmi and Gibson 2010) that has an almost identical excitation/emission maxima. Furthermore plobRFP has only 28% sequence identity with *Aequorea victoria* GFP (GenBank no. P42212) (Prasher et al. 1992). Phylogenetic analysis shows that plobRFP clusters with pporRFP and is a member of Clade B previously established in the coral FP phylogeny established by Alieva et al. (2008) (Online Resource 1, Fig. S.1, S.2). Protein modelling (SWISS-MODEL, (Schwede et al. 2003)) suggests that all of the secondary structures shared by GFP-like proteins (Yang et al. 1996; Ormo et al. 1996) are conserved in plobRFP (Fig. 3), i.e., tripeptide chromophore with conserved amino acids YG, 4 α-helixes, and 11 β-sheets.

Spectral properties of plobRFP

The purified recombinant plobRFP protein solution has a pink-purple coloration under brightfield illumination (Fig. 1c). Recombinant plobRFP (in PBS) has a wide absorption peak at 576 nm with shoulders at 542 nm and 502 nm (Fig. 4). A maximal red emission signal of 614 nm is produced when excited by green light (Ex. max: 578 nm) (Fig. 4). Spectra collected from the pink-pigmented *P. lobata* tissues produced a nearly identical emission peak (Fig. 4 *inset*). The mature plobRFP has a high molar extinction coefficient of 84,000 $M^{-1}cm^{-1}$ at its 578 nm excitation maximum (Fig. 4; Table 1). The excitation and emission profiles of the recombinant plobRFP and cresyl violet are similar, making this dye a useful reference standard in determining the comparative quantum yield of plobRFP (Online Resource 1, Fig. S.3). The (QY) of plobRFP was determined to be 0.74 using cresyl violet in methanol as a reference standard (Table 1). The inherent fluorescent brightness of plobRFP, the product of its MEC and QY, is 62.16.

Oligomeric status and aggregation of plobRFP

The “pseudo-native” state of plobRFP was evaluated using SDS-PAGE. The term pseudo-native is used to describe the un-heated protein sample as most GFP-like proteins do not

denature, i.e., they maintain oligomeric state and fluorescence in the presence of SDS at room temperature (Ward 2006; Baird et al. 2000). The un-heated pseudo-native plobRFP maintained its native fluorescence (Fig. 5a, b). Analysis by SDS-PAGE demonstrated that the recombinant protein forms obligate tetramers and has a strong tendency to aggregate. The oligomeric status of plobRFP is suggested by the migration of a very faint fluorescent band in the native sample to approximately the same location in the gel as the tetramer of recombinant DsRed2 (~71 KDa) (Fig. 5a, indicated by arrow). The less mobile and much more intense band of the native sample that remains in the stacking gel (within region marked by upper bracket, Fig. 5) may be explained by the tendency of plobRFP molecules to form and exist in higher order oligomeric forms (aggregation). Denatured (heated) plobRFP loses all fluorescence and migrates to approximately the same location (~35 kDa) as that of native GFP (a monomer), (Fig. 5c).

pH and photostability

The recombinant plobRFP is stable across a broad pH range (pH 2.5- 11.0). Most notably, plobRFP maintains >70% of its maximal fluorescence as well as its emission profile when incubated in an acidic pH of 2.5 (Fig. 6a). The recombinant plobRFP exhibits the highest fluorescence intensity at pH 3.5. At the most acidic pH examined (pH 1.0) plobRFP demonstrated an absorption increase in the 380 nm band along with a loss of the 576 and 455 nm absorption bands (Online Resource 1, Fig. S.4). This absorbance spectrum is characteristic of DsRed-type FPs and represents the protonated RFP chromophore in which all acylimine bonds have been reduced (Gross et al. 2000). Alkaline denaturation of plobRFP was observed at pH 13 and was represented by an increase in the 455 nm absorption band, equivalent to the alkaline denatured GFP chromophore (Ward 2006), and a decrease of the 576 nm absorption band (Online Resource 1, Fig. S.4).

The photostability of plobRFP and recombinant DsRed2 (in PBS) were tested under identical intense lighting conditions of 2,390 µmol $m^{-2}s^{-1}$ of PAR, ~1.5X greater than that of direct sunlight. Only 10% of this light intensity was required to detect the emission signal of plobRFP *in vivo* (in the coral tissue). Under the test conditions, the time for plobRFP to photobleach to 50% of its maximal emission intensity was 80 seconds compared to 45 seconds for DsRed2 (Fig. 6B). The rates of photobleaching for plobRFP and DsRed2 are fastest at the start of exposure, with the initial rate of bleaching for DsRed2 more exponential than plobRFP; following 50% loss of its original fluorescence intensity, plobRFP yields a photobleaching rate similar to DsRed2 (Fig. 6b).

Discussion

A number of fluorescent proteins with emission signals represented along the entire visible spectrum have been cloned from coral species. Although *in situ* spectral surveys of FPs in corals have described a red-emitting class of proteins with emission maxima reaching into the far-red region of the spectrum (Em: 620 nm) (Dove et al. 2001; Salih et al. 2000; Mazel et al. 2003; Oswald et al. 2007) prior to this study, only two red fluorescent proteins emitting at wavelengths greater than 600 nm had been cloned from anthozoans, and both were from anemones: eqFP611 from *Entacmaea quadricolor* (Em. max: 611 nm) (Wiedenmann et al. 2002) and NvFP-7R from *Nematostella vectensis* (Em. max: 613 nm) (Ikmi and Gibson 2010). Other than a dimly-emitting chromoprotein with faint red fluorescence, eforCP/RFP (Em. max:

609 nm), from *Echinopora forskaliana* (Alieva et al. 2008), no reef-building or scleractinian coral species have yielded true FPs with emission wavelengths greater than 600 nm.

In this study, a novel far-red emitting FP, plobRFP, was cloned, expressed, and biochemically characterized from the pink-pigmented tissues of the stony coral *Porites lobata*. The full length cDNA encodes a 233 amino acid protein, and the recombinantly expressed plobRFP exhibits a distinct bright red emission signal of 614 nm (Ex. max: 578 nm), with a high molar extinction coefficient (84,000 $M^{-1}cm^{-1}$) and quantum yield (0.74) this makes the emission signal of plobRFP the furthest red-shifted of all naturally occurring FPs cloned from scleractinian coral species. Furthermore, the brightness of plobRFP is significantly greater than any of the previously cloned anthozoan RFPs with emission wavelengths greater than 600 nm. Sequence analysis of plobRFP suggests that its unique spectral properties may reflect an equally unique chromophore arrangement.

The closest known homolog of plobRFP is pporRFP isolated from *Porites porites* with a maximal excitation of 578 nm and emission of 595 nm (Alieva et al. 2008). Overall, these closely related FPs share 79% amino acid sequence identity and both contain the Met-Tyr-Gly (MYG) tripeptide chromophore. While the MYG tripeptide can form chromophore structures that produce a range of emission signals (177 nm emission range) (Day and Davidson 2009), we predict the MYG tripeptide of plobRFP most likely matures into a variant of the DsRed-like chromophore type. Like other anthozoan FPs with the MYG DsRed type chromophore (pporRFP, eqFP611, eforCP/RFP)(Alieva et al. 2008; Wiedenmann et al. 2002; Petersen et al. 2003), plobRFP has a broad (defined as 50-60 nm spectral width) emission spectrum peaking in the 570-620 nm emission range and plobRFP exhibits alkaline and acid denaturation behavior characteristic of the DsRed type chromophore (Gross et al. 2000). Notably, though NvFP-7R has almost identical excitation and emission spectra (Ex. max: 578 nm; Em. max: 613 nm), it contains a Ser-Tyr-Gly (SYG) chromophore, the tripeptide combination characteristic of the *Aequorea victoria* GFP chromophore (Prasher et al. 1992). Thus, plobRFP and NvFP-7R represent entirely different alternatives for producing similar emission profiles and provide an example of convergent molecular evolution, a previously identified force shaping the evolution of red fluorescent proteins in the anthozoan GFP-like protein family (Shagin et al. 2004).

DsRed-like chromophores can exist in either *cis* or *trans* conformations. Most highly fluorescent RFP chromophores, with quantum yields between 0.49 and 0.70, are configured in a *cis* planar structure (Wall et al. 2000; Yarbrough et al. 2001), whereas the *trans* non-planar DsRed-like chromophore is exclusively represented in non-fluorescent chromoproteins (Prescott et al. 2003; Pakhomov et al. 2006; Chan et al. 2006). The unique chromophore of eqFP611 exists in a *trans* arrangement (Petersen et al. 2003) similar to that of non-fluorescent chromoproteins. The co-planarity of eqFP611 in the *trans* conformation facilitates fluorescence, albeit with a slightly lower quantum yield (QY: 0.45) (Wiedenmann et al. 2002) than DsRed (QY: 0.79) (Baird et al. 2000) and other RFPs in *cis* planar conformation. For FPs, a general trade-off appears to exist between longer wavelength emission signals and brightness. RFPs with DsRed-type chromophores in *cis* conformation produce a bright emission signal yet tend to emit below 600 nm (Alieva et al. 2008). Whereas in the less bright eqFP611, the *trans* co-planar arrangement of the chromophore and unique environment in the β-barrel lead to a red-shifted emission maximum of 611 nm (Petersen et al. 2003). Additionally, NvFP-7R and eforRFP/CP,

whose chromophore structures are not fully characterized, have far-red emission signals of 613 nm and 609 nm but have very low QYs (0.09 and 0.16, respectively).

Though the further red-shifted emission maximum of plobRFP is most similar to that of eqFP611, with the MYG DsRed-like chromophore in the *trans* coplanar conformation, and eforCP/RFP that likely adopts a similar configuration, the amino acid residues in several key positions controlling chromophore isomerization, are more typical of RFPs with DsRed-like chromophores in the *cis* conformation. Specifically, the amino acids in position 148 and 165 (numbered in accordance with *A. victoria* GFP alignment; highlighted in Fig. 3), which directly contact with the fluorophore, are critical in determining *cis/trans* conformation. Hydrophilic amino acids in position 165 can form a hydrogen bond with the hydroxyl group of the tyrosine of the chromophore and stabilize the *trans* conformation. Our sequence analysis indicates plobRFP contains the hydrophobic amino acid valine in position 165, which would destabilize *trans* conformation. Additionally, plobRFP contains a serine in position 148, which is conserved among most highly fluorescent RFPs; the polar serine is capable of forming hydrogen bonds which stabilize *cis* conformation (Gurskaya et al. 2001; Bulina et al. 2002). Therefore, we predict the MYG DsRed type chromophore of plobRFP exists in a *cis* conformation, which would explain the strong brightness of plobRFP with a QY of 0.74 compared to that of eqFP611 (QY: 0.45) (Wiedenmann et al. 2002)and eforCP/RFP (QY: 0.16) (Alieva et al. 2008).

Intriguingly, the closest homolog (pporRFP) of plobRFP contains the same amino acids in the previously discussed key positions impacting chromophore conformation. However, pporRFP produces an emission maximum of 595 nm (Alieva et al. 2008) compared to that of 614 nm for plobRFP. Therefore, it is likely that additional residues influencing the environment within the β-barrel and interacting with the chromophore facilitate the 19 nm red shift in emission. For example, potential features that could influence the spectral shift include additional hydrogen bonding to the N-acylimine of the chromophore, pi-stacking interactions, or the presence of hydrophobic residues surrounding the chromophore, properties responsible for the red-shifted emission profiles of far-red FPs engineered from the DsRed protein (reviewed by Subach et al. (2011)). Notably, the bright and further red-shifted RFPs commercially available are essentially derived from several natural RFPs, DsRed (Matz et al. 1999), eqFP611 (Wiedenmann et al. 2002), and the closely related homolog, eqFP578 (Merzlyak et al. 2007) (reviewed by Day and Davidson (2009)). The isolation of plobRFP with both the brightness of DsRed and the further red-shifted emission of eqFP611 provides a unique template for engineering FPs with unknown novel photophysical properties.

The sequence of plobRFP can also provide insight on the molecular evolution of the anthozoan GFP-like protein family. Molecular phylogenies previously built with FP amino acid sequences demonstrate that the majority of GFP-like proteins distribute in groups that mirror the taxonomy of their host organisms (Labas et al. 2002; Alieva et al. 2008; Shagin et al. 2004). Phylogenetic analysis places plobRFP into Clade B, of the previously constructed anthozoan FP phylogenetic tree (Alieva et al. 2008). Clade B is mostly comprised of chromoproteins, but also includes DsRed-like FPs and one cyan FP. The cloned plobRFP falls as a sister group to pporRFP, previously placed in the most basal position of Clade B and clusters with a unique chromo/red FP, eforCP/RFP. As noted by Alieva et al. (2008), Clade B represents a paralogous group of GFP-like proteins that while other FP genes were present in the genomes of their host species, its members were maintained likely due to special functional roles. The association of plobRFP,

pporRFP, and several CPs in Clade B with abnormal tissue pigmentation responses suggests that their role in these responses could be a selective factor shaping the maintenance of these clade members in their host species genomes.

Herein, we describe similar histological observations in *Porites lobata* as those documented by Palmer et al. (2008, 2009b). We document the localization of plobRFP to the surface body wall as well as a concentration of melanin-containing cells (putative amoebocytes) beneath the epidermal tissue layer and flanking regions of lysing tissue. Although the association of plobRFP alone is not sufficient or direct evidence to suggest an immune response, given the nascent state of science regarding coral innate immunity as well as similar observations reported by Palmer et al. (2008, 2009b) and D'Angelo et al. (2012) of poritid coral species, this protein could either be an indicator of an immune response or mechanistically involved in the immune response of this species. The isolation of plobRFP provides a valuable tool for further evaluating the recently proposed antioxidant role for TPR-associated FPs as well the regulation of plobRFP in response to various inducers. The coding sequences can now be incorporated into quantitative expression studies, and the pure recombinant plobRFP will be useful in functional assays, such as the antioxidant H_2O_2 scavenging assay employed by Palmer et al. (2009a) with recombinant *Acropora* chromoproteins. Once the pathology of the pink-pigmentation response is more precisely defined, the bright visible signal of plobRFP in the impacted tissues offers a potential visual diagnostic tool, as well as a molecular biomarker for monitoring coral health in the field.

As many commercially available RFPs suffer from diminished brightness, we sought to biochemically characterize the recombinantly expressed plobRFP in an effort to comment on its biotechnological application. The recombinant plobRFP *in vitro* demonstrated high pH and photostability, likely a result of its quaternary structure; tight packing of plobRFP tetramers in higher order aggregates could provide protection to the chromophore. Across a broad pH range (pH 2.5-11.0), plobRFP maintained >70% of its maximal fluorescence. The majority of natural FPs and their derivatives lose approximately 50% of their emission intensity outside the pH range of 4.0–10.0 (Kneen et al. 1998; Baird et al. 2000; Shaner et al. 2005). The distinct stability of plobRFP in extreme pHs could be useful for imaging in acidic cellular compartments or physiological processes involving a shift in pH. A review by Piatkevich et al. (2010) evaluating the photostability of >20 known natural and optimized RFPs following the method proposed by Shaner et al. (2005) reported that DsRed is the second most photostable RFP of all RFPs surveyed. In our preliminary studies on the photostability of plobRFP, we observed that plobRFP appears to be more photostable than DsRed. Though our measures of photostability were not corrected for some of the normalization factors described by Shaner et al. (2005), the two RFPs compared were measured under identical conditions and have similar brightness properties. The crystal structure of plobRFP needs to be resolved in order to comment on residues or modifications contributing to the observed photostability of plobRFP. This is due to the fact that a consequential relationship between FP structure and photostability is still not well defined. In fact, the current approach towards improving FP photostability involves screening large libraries of variants for increased photostability readouts rather than direct, rationale-based mutations to specific residues of the protein (Wiens et al. 2018; Dean et al. 2015; Shaner et al. 2008). This is partially due to the fact that photobleaching can occur through different mechanisms, even for FPs with similar chromophores. For some optimized RFPs

photostability has been improved by amino acid substitutions that directly or indirectly prevent oxidation of the chromophore (Shaner et al. 2008; Dean et al. 2015), yet, for others, oxidation of a cysteine residue close to the chromophore has been shown to actually increase photostability (Ren et al. 2016). SDS-PAGE analysis of plobRFP revealed that, like other natural RFPs, plobRFP may exist as an obligate tetramer and has tendency to aggregate. While tetrameric FPs have been used successfully in certain imaging applications (Wiedenmann et al. 2009), the aggregation tendency of plobRFP is the most limiting feature of this RFP; recombinant FP aggregates can be toxic to host cells and impact the resolution of fluorescent images (Katayama et al. 2008). Mutagenesis strategies that generally focus on targeting electrostatic interactions on the surface of FP molecules have been developed (Yanushevich et al. 2002; Wannier et al. 2018) and could be successfully applied to alleviate this behavior.

Conclusions

Herein we report the cloning and characterization of a novel RFP, plobRFP, from a cultured *Porites lobata* specimen exhibiting the distinct pink tissue pigmentation response reported previously for *Porites* species. The bright 614 nm emission signal of plobRFP confirms that we have isolated the RFP responsible for the red fluorescence observed *in vivo*. The connection of the bright distinct red emission to a suggested innate immune response in *P. lobata* implies plobRFP may have application as a useful diagnostic tool for monitoring coral health. Additionally, we propose the bright red-shifted emission signal of plobRFP may be the result of a uniquely configured chromophore. This suggests plobRFP may serve as a template for optimizing and developing FPs that will serve to fill the gap for needed bright far red-shifted emission. Furthermore, plobRFP itself may serve as a valuable fluorescent reporter given its stability and spectral properties.

Acknowledgements

We wish to acknowledge the technical support of James H. Nicholson for his assistance with microscopy and image processing; Carl Miller for the maintenance of coral specimens in the NCCOS coral culture facility; and Athena Burnett and Dorothy Howard for coral tissue processing and histology. We would also like to thank Chroma Technology Corp (Bellow Falls, VT) for the donation of custom excitation and emission filters.

Conflict of Interest

The authors declare they have no conflict of interest.

NOAA Disclaimer

This publication does not constitute an endorsement of any commercial product or intend to be an opinion beyond scientific or other results obtained by the National Oceanic and Atmospheric Administration (NOAA). No reference shall be made to NOAA, or this publication furnished by NOAA, to any advertising or sales promotion, which would indicate or imply that NOAA recommends or endorses any proprietary product mentioned herein, or which has as its purpose an interest to cause the advertised product to be used or purchased because of this publication.

Author Contributions

C.M.W. and S.B.G. conceived the study. C.M.W., S.B.G., and L.A.M. were in charge of overall direction and planning. M.C.B. planned and carried out the experiments and wrote the manuscript with input from all authors. E.C.P. conducted and interpreted the histology. All authors discussed the results and contributed to the final manuscript.

References

Aeby G (2003) Corals in the genus Porites are susceptible to infection by a larval trematode. Coral Reefs 22:216-216

Alieva NO, Konzen KA, Field SF, Meleshkevitch EA, Hunt ME, Beltran-Ramirez V, Miller DJ, Wiedenmann J, Salih A, Matz MV (2008) Diversity and evolution of coral fluorescent proteins. PLoS One 3:e2680

Altschul SF, Gish W, Miller W, Myers EW, Lipman DJ (1990) Basic local alignment search tool. J Mol Biol 215:403-10

Baird GS, Zacharias DA, Tsien RY (2000) Biochemistry, mutagenesis, and oligomerization of DsRed, a red fluorescent protein from coral. Proc Natl Acad Sci U S A 97:11984-9

Benzoni F, Galli P, Pichon M (2010) Pink spots on Porites: not always a coral disease. Coral Reefs 29:153-153

Bongiorni L, Rinkevich B (2005) The pink-blue spot syndrome in Acropora eurystoma (Eilat, Red Sea): A possible marker of stress? Zoology 108:247-256

Bou-Abdallah F, Chasteen ND, Lesser MP (2006) Quenching of superoxide radicals by green fluorescent protein. Biochim Biophys Acta 1760:1690-5

Brouwer AM (2011) Standards for photoluminescence quantum yield measurements in solution (IUPAC Technical Report). Pure Appl Chem 83:2213-2228

Bulina ME, Chudakov DM, Mudrik NN, Lukyanov KA (2002) Interconversion of Anthozoa GFP-like fluorescent and non-fluorescent proteins by mutagenesis. BMC Biochem 3:7

Chan MC, Karasawa S, Mizuno H, Bosanac I, Ho D, Prive GG, Miyawaki A, Ikura M (2006) Structural characterization of a blue chromoprotein and its yellow mutant from the sea anemone Cnidopus japonicus. J Biol Chem 281:37813-9

Chudakov DM, Matz MV, Lukyanov S, Lukyanov KA (2010) Fluorescent proteins and their applications in imaging living cells and tissues. Physiol Rev 90:1103-63

D'angelo C, Denzel A, Vogt A, Matz MV, Oswald F, Salih A, Nienhaus GU, Wiedenmann J (2008) Blue light regulation of host pigment in reef-building corals. Mar Ecol Prog Ser 364:97-106

D'angelo C, Smith E, Oswald F, Burt J, Tchernov D, Wiedenmann J (2012) Locally accelerated growth is part of the innate immune response and repair mechanisms in reef-building corals as detected by green fluorescent protein (GFP)-like pigments. Coral Reefs 31:1045-1056

Day RN, Davidson MW (2009) The fluorescent protein palette: tools for cellular imaging. Chem Soc Rev 38:2887-921

Dean KM, Lubbeck JL, Davis LM, Regmi CK, Chapagain PP, Gerstman BS, Jimenez R, Palmer AE (2015) Microfluidics-based selection of red-fluorescent proteins with decreased rates of photobleaching. Integr Biol (Camb) 7:263-73

Dove S, Hoegh-Guldberg O, Ranganathan S (2001) Major colour patterns of reef-building corals are due to a family of GFP-like proteins. Coral Reefs 19:197-204

Field SF, Bulina MY, Kelmanson IV, Bielawski JP, Matz MV (2006) Adaptive evolution of multicolored fluorescent proteins in reef-building corals. J Mol Evol 62:332-9

Gross LA, Baird GS, Hoffman RC, Baldridge KK, Tsien RY (2000) The structure of the chromophore within DsRed, a red fluorescent protein from coral. Proc Natl Acad Sci U S A 97:11990-5
Gruber DF, Kao H-T, Janoschka S, Tsai J, Pieribone VA (2008) Patterns of fluorescent protein expression in scleractinian corals. Biol Bull 215:143-154
Guindon S, Gascuel O (2003) A simple, fast, and accurate algorithm to estimate large phylogenies by maximum likelihood. Syst Biol 52:696-704
Gurskaya NG, Fradkov AF, Terskikh A, Matz MV, Labas YA, Martynov VI, Yanushevich YG, Lukyanov KA, Lukyanov SA (2001) GFP-like chromoproteins as a source of far-red fluorescent proteins. FEBS Lett 507:16-20
Heim R, Prasher DC, Tsien RY (1994) Wavelength mutations and posttranslational autoxidation of green fluorescent protein. Proc Natl Acad Sci U S A 91:12501-4
Hunt ME, Scherrer MP, Ferrari FD, Matz MV (2010) Very bright green fluorescent proteins from the Pontellid copepod Pontella mimocerami. PLoS One 5:e11517
Ikmi A, Gibson MC (2010) Identification and in vivo characterization of NvFP-7R, a developmentally regulated red fluorescent protein of Nematostella vectensis. PLoS One 5:e11807
Isak SJ, Eyring EM (1992) Fluorescence quantum yield of cresyl violet in methanol and water as a function of concentration. J Phys Chem 96:1738-1742
Jones DT, Taylor WR, Thornton JM (1992) The rapid generation of mutation data matrices from protein sequences. Comput Appl Biosci 8:275-82
Katayama H, Yamamoto A, Mizushima N, Yoshimori T, Miyawaki A (2008) GFP-like proteins stably accumulate in lysosomes. Cell Struct Funct 33:1-12
Kawaguti S (1969) Effect of the green fluorescent pigment on the productivity of the reef corals. Micronesica 5:121
Kneen M, Farinas J, Li Y, Verkman A (1998) Green fluorescent protein as a noninvasive intracellular pH indicator. Biophys J 74:1591-1599
Labas YA, Gurskaya NG, Yanushevich YG, Fradkov AF, Lukyanov KA, Lukyanov SA, Matz MV (2002) Diversity and evolution of the green fluorescent protein family. Proc Natl Acad Sci U S A 99:4256-61
Laemmli UK (1970) Cleavage of structural proteins during the assembly of the head of bacteriophage T4. Nature 227:680-5
Lakowicz JR (2006) Principles of fluorescence spectroscopy. Springer Science & Business Media, New York
Levy O, Dubinsky Z, Achituv Y (2003) Photobehavior of stony corals: responses to light spectra and intensity. J Exp Biol 206:4041-9
Magde D, Brannon JH, Cremers TL, Olmsted J (1979) Absolute luminescence yield of cresyl violet. A standard for the red. J Phys Chem 83:696-699
Masuda H, Takenaka Y, Yamaguchi A, Nishikawa S, Mizuno H (2006) A novel yellowish-green fluorescent protein from the marine copepod, Chiridius poppei, and its use as a reporter protein in HeLa cells. Gene 372:18-25
Matz MV, Fradkov AF, Labas YA, Savitsky AP, Zaraisky AG, Markelov ML, Lukyanov SA (1999) Fluorescent proteins from nonbioluminescent Anthozoa species. Nat Biotechnol 17:969-73
Mazel CH, Lesser MP, Gorbunov MY, Barry TM, Farrell JH, Wyman KD, Falkowski PG (2003) Green-fluorescent proteins in Caribbean corals. Limnol Oceanogr 48:402-411
Merzlyak EM, Goedhart J, Shcherbo D, Bulina ME, Shcheglov AS, Fradkov AF, Gaintzeva A, Lukyanov KA, Lukyanov S, Gadella TW, Chudakov DM (2007) Bright monomeric red fluorescent protein with an extended fluorescence lifetime. Nat Methods 4:555-7
Nienhaus GU, Wiedenmann J (2009) Structure, dynamics and optical properties of fluorescent proteins: perspectives for marker development. Chemphyschem 10:1369-79

Ong WJ, Alvarez S, Leroux IE, Shahid RS, Samma AA, Peshkepija P, Morgan AL, Mulcahy S, Zimmer M (2011) Function and structure of GFP-like proteins in the protein data bank. Mol Biosyst 7:984-92
Ormo M, Cubitt AB, Kallio K, Gross LA, Tsien RY, Remington SJ (1996) Crystal structure of the Aequorea victoria green fluorescent protein. Science 273:1392-5
Oswald F, Schmitt F, Leutenegger A, Ivanchenko S, D'angelo C, Salih A, Maslakova S, Bulina M, Schirmbeck R, Nienhaus GU, Matz MV, Wiedenmann J (2007) Contributions of host and symbiont pigments to the coloration of reef corals. FEBS J 274:1102-9
Pakhomov AA, Pletneva NV, Balashova TA, Martynov VI (2006) Structure and reactivity of the chromophore of a GFP-like chromoprotein from Condylactis gigantea. Biochemistry 45:7256-64
Palmer CV, Modi CK, Mydlarz LD (2009a) Coral fluorescent proteins as antioxidants. PloS One 4:e7298
Palmer CV, Mydlarz LD, Willis BL (2008) Evidence of an inflammatory-like response in non-normally pigmented tissues of two scleractinian corals. Proc Biol Sci 275:2687-93
Palmer CV, Roth MS, Gates RD (2009b) Red fluorescent protein responsible for pigmentation in trematode-infected Porites compressa tissues. Biol Bull 216:68-74
Petersen J, Wilmann PG, Beddoe T, Oakley AJ, Devenish RJ, Prescott M, Rossjohn J (2003) The 2.0-A crystal structure of eqFP611, a far red fluorescent protein from the sea anemone Entacmaea quadricolor. J Biol Chem 278:44626-31
Piatkevich KD, Efremenko EN, Verkhusha VV, Varfolomeev SD (2010) Red fluorescent proteins and their properties. Russian Chemical Reviews 79:243
Prasher DC, Eckenrode VK, Ward WW, Prendergast FG, Cormier MJ (1992) Primary structure of the Aequorea victoria green-fluorescent protein. Gene 111:229-33
Prescott M, Ling M, Beddoe T, Oakley AJ, Dove S, Hoegh-Guldberg O, Devenish RJ, Rossjohn J (2003) The 2.2 A crystal structure of a pocilloporin pigment reveals a nonplanar chromophore conformation. Structure 11:275-84
Ravindran J, Raghukumar C (2006) Pink-line syndrome, a physiological crisis in the scleractinian coral Porites lutea. Mar Biol 149:347-356
Ren H, Yang B, Ma C, Hu YS, Wang PG, Wang L (2016) Cysteine Sulfoxidation Increases the Photostability of Red Fluorescent Proteins. ACS Chem Biol 11:2679-2684
Saitou N, Nei M (1987) The neighbor-joining method: a new method for reconstructing phylogenetic trees. Mol Biol Evol 4:406-25
Salih A, Larkum A, Cox G, Kuhl M, Hoegh-Guldberg O (2000) Fluorescent pigments in corals are photoprotective. Nature 408:850-3
Sanger F, Nicklen S, Coulson AR (1977) DNA sequencing with chain-terminating inhibitors. Proc Natl Acad Sci U S A 74:5463-5467
Schwede T, Kopp J, Guex N, Peitsch MC (2003) SWISS-MODEL: An automated protein homology-modeling server. Nucleic Acids Res 31:3381-5
Shagin DA, Barsova EV, Yanushevich YG, Fradkov AF, Lukyanov KA, Labas YA, Semenova TN, Ugalde JA, Meyers A, Nunez JM, Widder EA, Lukyanov SA, Matz MV (2004) GFP-like proteins as ubiquitous metazoan superfamily: evolution of functional features and structural complexity. Mol Biol Evol 21:841-50
Shaner NC, Lin MZ, Mckeown MR, Steinbach PA, Hazelwood KL, Davidson MW, Tsien RY (2008) Improving the photostability of bright monomeric orange and red fluorescent proteins. Nat Methods 5:545-51
Shaner NC, Steinbach PA, Tsien RY (2005) A guide to choosing fluorescent proteins. Nat Methods 2:905-9

Shcherbo D, Merzlyak EM, Chepurnykh TV, Fradkov AF, Ermakova GV, Solovieva EA, Lukyanov KA, Bogdanova EA, Zaraisky AG, Lukyanov S, Chudakov DM (2007) Bright far-red fluorescent protein for whole-body imaging. Nat Methods 4:741-6

Shepard AR, Rae JL (1997) Magnetic bead capture of cDNAs from double-stranded plasmid cDNA libraries. Nucleic Acids Res 25:3183-5

Shikina S, Chiu YL, Chung YJ, Chen CJ, Lee YH, Chang CF (2016) Oocytes express an endogenous red fluorescent protein in a stony coral, Euphyllia ancora: a potential involvement in coral oogenesis. Sci Rep 6:25868

Sievers F, Wilm A, Dineen D, Gibson TJ, Karplus K, Li W, Lopez R, Mcwilliam H, Remmert M, Soding J, Thompson JD, Higgins DG (2011) Fast, scalable generation of high-quality protein multiple sequence alignments using Clustal Omega. Mol Syst Biol 7:539

Smith EG, D'angelo C, Salih A, Wiedenmann J (2013) Screening by coral green fluorescent protein (GFP)-like chromoproteins supports a role in photoprotection of zooxanthellae. Coral Reefs 32:463-474

Stepanenko OV, Stepanenko OV, Shcherbakova DM, Kuznetsova IM, Turoverov KK, Verkhusha VV (2011) Modern fluorescent proteins: from chromophore formation to novel intracellular applications. Biotechniques 51:313-4, 316, 318

Subach FV, Piatkevich KD, Verkhusha VV (2011) Directed molecular evolution to design advanced red fluorescent proteins. Nat Methods 8:1019-26

Tamura K, Stecher G, Peterson D, Filipski A, Kumar S (2013) MEGA6: Molecular Evolutionary Genetics Analysis version 6.0. Mol Biol Evol 30:2725-9

Tsien RY (1998) The green fluorescent protein. Annu Rev Biochem 67:509-44

Ugalde JA, Chang BS, Matz MV (2004) Evolution of coral pigments recreated. Science 305:1433

Vogt A, D'angelo C, Oswald F, Denzel A, Mazel CH, Matz MV, Ivanchenko S, Nienhaus GU, Wiedenmann J (2008) A green fluorescent protein with photoswitchable emission from the deep sea. PLoS One 3:e3766

Wall MA, Socolich M, Ranganathan R (2000) The structural basis for red fluorescence in the tetrameric GFP homolog DsRed. Nat Struct Biol 7:1133-8

Wannier TM, Gillespie SK, Hutchins N, Mcisaac RS, Wu SY, Shen Y, Campbell RE, Brown KS, Mayo SL (2018) Monomerization of far-red fluorescent proteins. Proc Natl Acad Sci U S A 115:E11294-E11301

Ward WW (2006) In: Chalfie M, Kain SR (eds) Green fluorescent protein: properties, applications, and protocols, 2nd edn. John Wiley and Sons, New York

Wiedenmann J, Ivanchenko S, Oswald F, Nienhaus GU (2004) Identification of GFP-like proteins in nonbioluminescent, azooxanthellate anthozoa opens new perspectives for bioprospecting. Mar Biotechnol (NY) 6:270-7

Wiedenmann J, Oswald F, Nienhaus GU (2009) Fluorescent proteins for live cell imaging: opportunities, limitations, and challenges. IUBMB Life 61:1029-42

Wiedenmann J, Schenk A, Rocker C, Girod A, Spindler KD, Nienhaus GU (2002) A far-red fluorescent protein with fast maturation and reduced oligomerization tendency from Entacmaea quadricolor (Anthozoa, Actinaria). Proc Natl Acad Sci U S A 99:11646-51

Wiens MD, Hoffmann F, Chen Y, Campbell RE (2018) Enhancing fluorescent protein photostability through robot-assisted photobleaching. Integr Biol (Camb) 10:419-428

Yang F, Moss LG, Phillips GN, Jr. (1996) The molecular structure of green fluorescent protein. Nat Biotechnol 14:1246-51

Yanushevich YG, Staroverov DB, Savitsky AP, Fradkov AF, Gurskaya NG, Bulina ME, Lukyanov KA, Lukyanov SA (2002) A strategy for the generation of non-aggregating mutants of Anthozoa fluorescent proteins. FEBS Lett 511:11-4

Yarbrough D, Wachter RM, Kallio K, Matz MV, Remington SJ (2001) Refined crystal structure of DsRed, a red fluorescent protein from coral, at 2.0-A resolution. Proc Natl Acad Sci U S A 98:462-7

Table

Table 1 Photophysical properties of anthozoan red fluorescent proteins

Protein	Excitation maximum (nm)	Emission maximum (nm)	Extinction coefficient ($M^{-1}cm^{-1}$)[a]	Quantum yield (QY)	Brightness[b]	Reference
plobRFP	578	614	84,000	0.74	62.16	this work
pporRFP	578	595	94,900	0.54	51.25	(Alieva et al. 2008)
DsRed	558	583	75,000	0.79	59.25	(Baird et al. 2000)
epFP611	559	611	116,000	0.45	52.20	(Wiedenmann et al. 2002)
eforCP/RFP	589	609	111,300	0.16	17.81	(Alieva et al. 2008)
NvFP-7R	578	613	---	0.09	---	(Ikmi and Gibson 2010)

[a] Concentration of the red chromophore determined by the alkaline denaturation method (Gross et al. 2000)

[b] Brightness is determined as a product of quantum yield and molar extinction coefficient divided by 1000

Figure Captions

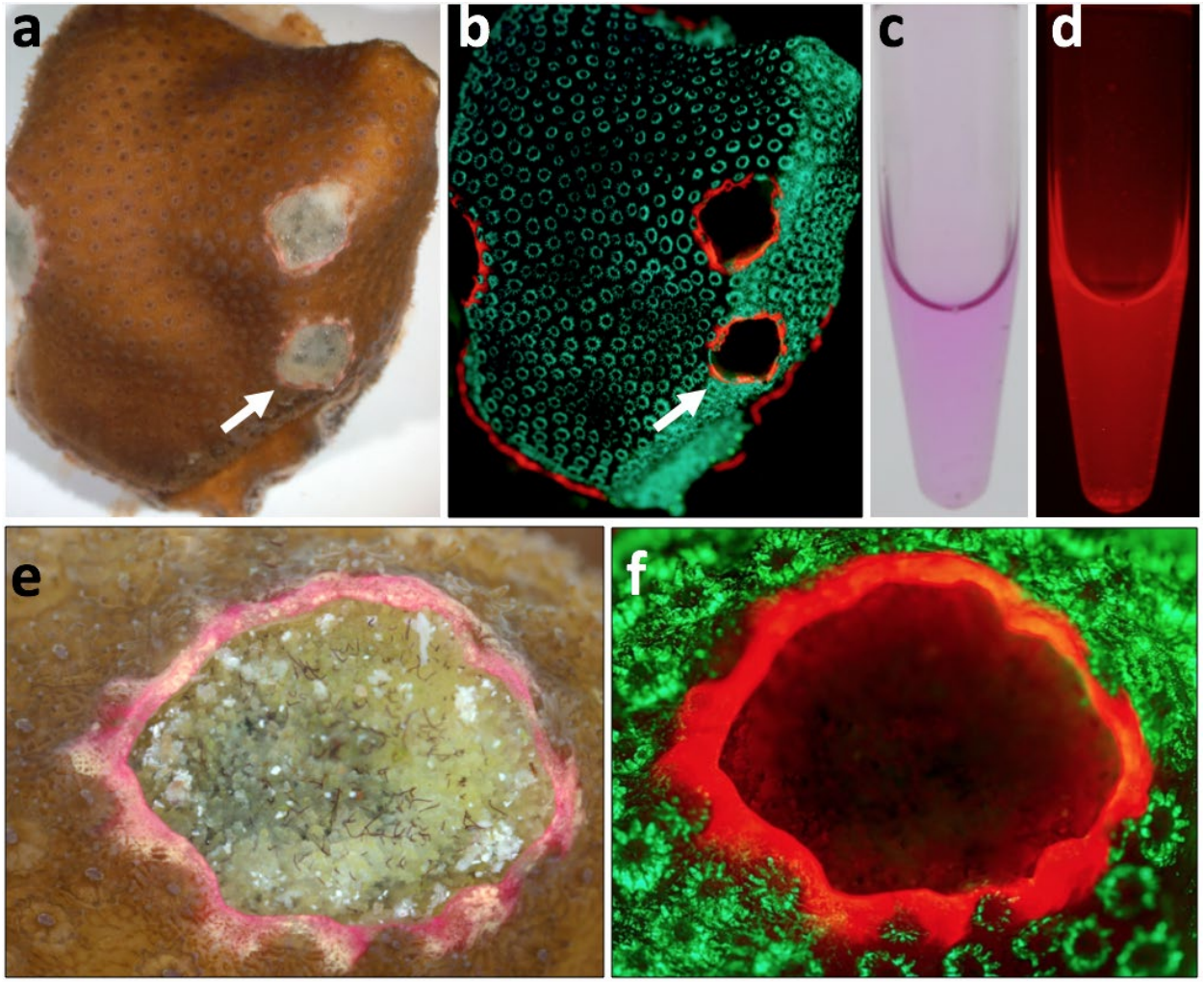

Fig. 1 Identification of a novel red fluorescent protein (plobRFP) in *Porites lobata* Pink pigmentation in *P. lobata* surrounding circular lesions in the coral tissue visualized under brightfield illumination (a, e) and blue/green light excitation (b, f). Arrows (in a, b) indicate the lesion magnified in panels e and f. This lesion was approximately 6.5-7.5 cm in diameter. Brightfield (c) and green light illumination (d) of the purified recombinant plobRFP.

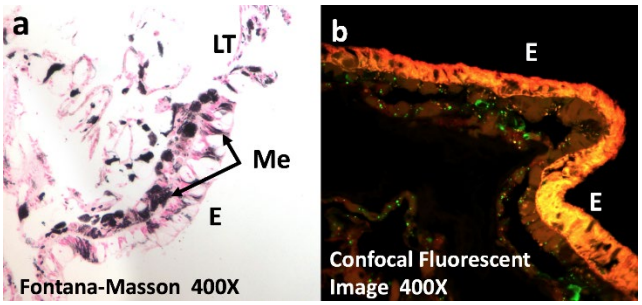

Fig. 2 Stained and fluorescent histological sections of tissue exhibiting the pink pigmentation response a) granular melanin-containing cells (amoebocytes) aligning along and infiltrating the epidermal layer; b) autofluorescence of plobRFP indicates localization to the epidermal tissue layer. E= epidermal tissue layer, LT= lysing tissue, Me= granular melanin-containing cells.

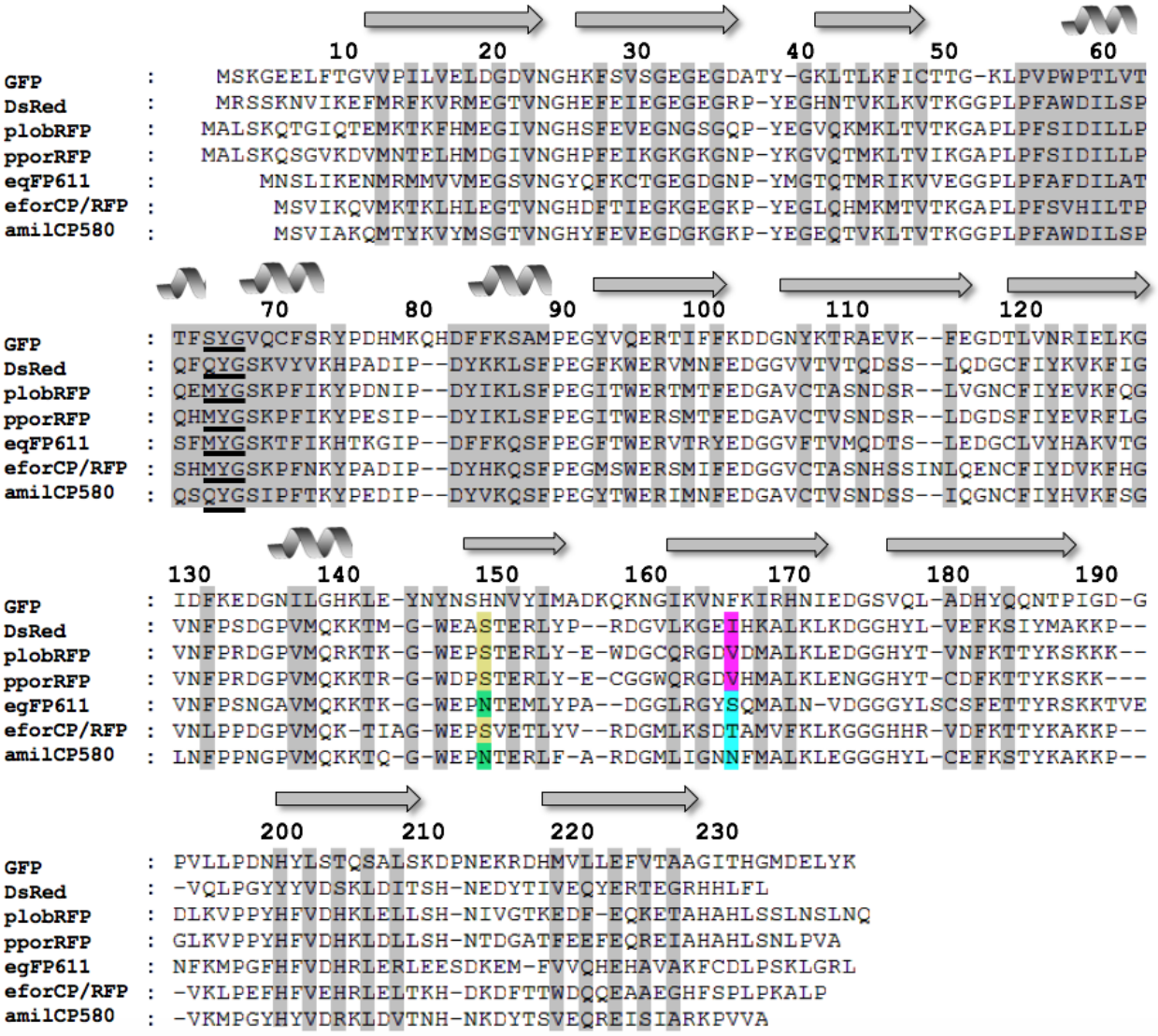

Fig. 3 Multiple alignment of amino acid sequences from coral fluorescent proteins, chromoproteins, and *Aequorea victoria* GFP The numbering above the sequences is based on *A. victoria* GFP. Predicted secondary structures are displayed above the sequences (alpha-helices and β-strands: arrows). Residues with side chains positioned within the interior of the β-barrel are shaded in grey. The tripeptide chromophore is underlined and key residues mentioned in the discussion are highlighted in yellow (*cis* stabilizing) and fuchsia/cyan (hydrophobic/hydrophilic).

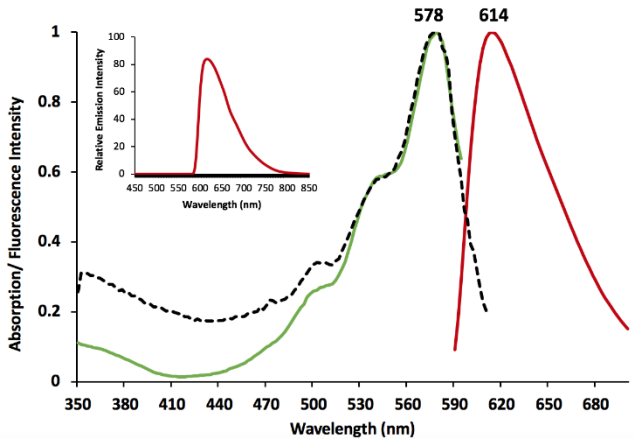

Fig. 4 Absorption, excitation, and emission spectra of plobRFP Absorption (dashed line), excitation (solid green), and emission (solid red) spectra were recorded from purified recombinant plobRFP in PBS. *Inset*: Emission spectrum collected from a pink-pigmented region of *P. lobata* tissue.

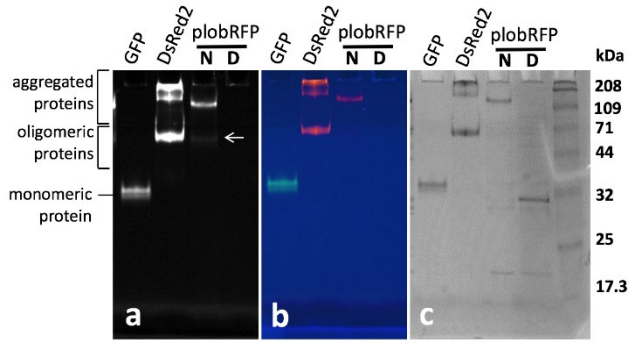

Fig. 5 Aggregation and oligomerization of recombinant plobRFP a,b) photographs of a 12.5% SDS-polyacrylamide gel taken with UV illumination. Both panel a (ethidium bromide filter) and panel b (no filter) demonstrate that the native FP samples maintain their fluorescence in the presence of SDS. c) photograph of the gel (white light illumination) after Coomassie Blue staining of all proteins. GFP and DsRed2 represent monomeric and tetrameric standards (respectively) for globule size. Standard molecular weight markers are to the right of the gels. Wells marked with an (N) denote unheated FP samples in their pseudo-native (non-denatured) states. Wells marked with a (D) indicate samples that were heated for 3 min (denatured) prior to being loaded onto the gel.

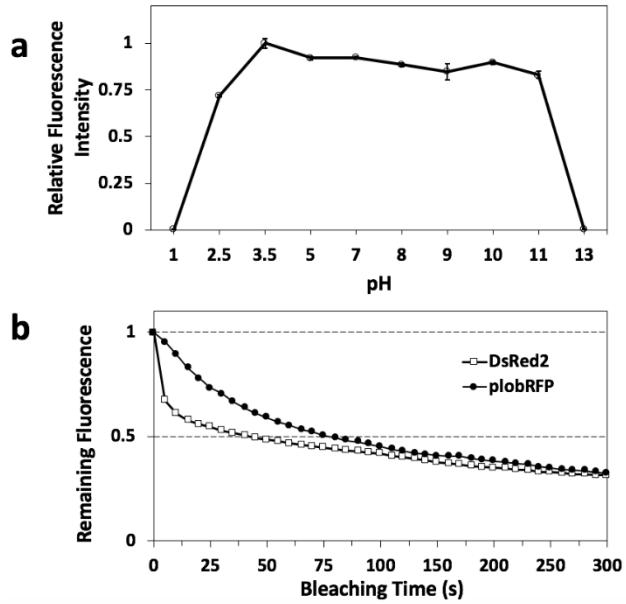

Fig. 6 Photostability and pH of plobRFP a) Fluorescent intensity of plobRFP (Ex: 578 nm; Em: 614 nm) recorded after 20 min of incubation in a range of pH buffers; each point represents an average of three replicate measurements (error bars: standard error of the mean). b) The photobleaching rate of plobRFP compared to the commercially available recombinant DsRed2 at equal concentration and under identical illumination conditions (Ex: 540 nm; PAR: 2,390 µmol $m^{-2}s^{-1}$).

Electronic Supplementary Material

Online Resource 1 (ESM_1.pdf) contains the following:

Table S.1 Degenerate primers homologous to conserved regions of Clade B GFP-like protein genes

Fig. S.1 Neighbor-joining tree of cnidarian fluorescent proteins

Fig. S.2 Maximum likelihood tree of cnidarian fluorescent proteins

Fig. S.3 Absorbance and emission spectra of plobRFP and the QY reference standard, cresyl violet

Fig. S.4 Effect of pH on the spectral properties of plobRFP